Study of the Xenon Mobility in the Two Forms of MIL-53(Al) Using Solid-State NMR Spectroscopy

Journal:	*The Journal of Physical Chemistry*
Manuscript ID	jp-2017-06006f.R2
Manuscript Type:	Article
Date Submitted by the Author:	31-Jul-2017
Complete List of Authors:	Giovine, Raynald; Universite Lille 1 Volkringer, Christophe; ENSC Lille, Springuel-Huet, Marie-Anne; Université P. et M. Curie, Laboratoire de Chimie de la Matière Condensée de Paris (cc 196) Nossov, Andrei; Université P. et M. Cuire, Laboratoire de Chimie de la Matière Condensée de Paris Blanc, Frédéric; University of Liverpool, Chemistry Trebosc, Julien; Université des Sciences et Technologies de Lille, UCCS - Unité de Catalyse et de Chimie du Solide Loiseau, Thierry; Unité de Catalyse et Chimie du Solide - UMR CNRS 8181, Université de Lille - USTL-ENSCL Amoureux, Jean-Paul; University of Lille, Chemistry Lafon, Olivier; Universite de Lille Nord de France, Unite de Catalyse et de Chimie du Solide Pourpoint, Frédérique; Univ. Lille Nord de France, UCCS

SCHOLARONE™
Manuscripts

1
2
3
4
5
6
7
8
9
10
11
12
13
14
15
16
17
18
19
20
21
22
23
24
25
26
27
28
29
30
31
32
33
34
35
36
37
38
39
40
41
42
43
44
45
46
47
48
49
50
51
52
53
54
55
56
57
58
59
60

Study of the Xenon Mobility in the Two Forms of MIL-53(Al) Using Solid-State NMR Spectroscopy

Raynald Giovine,[a] Christophe Volkringer,[a,b] Marie-Anne Springuel-Huet[c], Andrei Nossov[c] , Frédéric Blanc[d], Julien Trébosc,[a] Thierry Loiseau,[a] Jean-Paul Amoureux,[a,e] Olivier Lafon,[a,b] Frédérique Pourpoint*[a]

a Univ. Lille, CNRS, ENSCL, Centrale Lille, Univ. Artois, UMR 8181 - UCCS - Unité de Catalyse et Chimie du Solide, F-59000 Lille, France

b Institut Universitaire de France, 1 rue Descartes, 75231 Paris Cedex 5, France

c Sorbonne Universités, UPMC, Univ. Paris 06, CNRS, Collège de France, UMR 7574 –Laboratoire de Chimie de la Matière Condensée de Paris (LCMCP), 4 place Jussieu, F-75005 Paris, France

d Department of Chemistry and Stephenson Institute for Renewable Energy, University of Liverpool, Crown Street, Liverpool L69 7ZD, United Kingdom

e Bruker, Biospin, 34 rue de l'industrie, 67160 Wissembourg, France

Corresponding author: frederique.pourpoint@ensc-lille.fr

1

1
2
3
4
5
6
7
8
9
10
11
12
13
14
15
16
17
18
19
20
21
22
23
24
25
26
27
28
29
30
31
32
33
34
35
36
37
38
39
40
41
42
43
44
45
46
47
48
49
50
51
52
53
54
55
56
57
58
59
60

Abstract: The Al-based Metal-Organic Framework (MOF) MIL-53(Al) exhibits a structural transition between a large-pore (*lp*) form and a narrow-pore (*np*) one. Such change is induced by temperature, external pressure or the adsorption of guest molecules. ^{129}Xe solid-state NMR experiments under static and Magic-Angle Spinning (MAS) conditions have been used to study the *lp-np* transition in MIL-53(Al) initially loaded with xenon gas under a pressure of 5×10^4 Pa (at room temperature). The conversion of *lp* form into *np* one when the temperature decreases from 327 to 237 K and the reopening of the pores below 230 K are then observed. Furthermore, ^{1}H$\rightarrow^{129}$Xe Cross-Polarization under MAS (CP-MAS) experiments demonstrate the possibility to observe the *np* phase at $T \leq 230$ K, while the *lp* one is unseen because the xenon residence time is too short for successful cross-polarization transfer. Moreover even for the *np* phase at 199 K, the xenon atoms still exhibit significant motion on timescale faster than a few milliseconds. We prove the exchange of Xe atoms between the *lp* and *np* forms at room temperature with the two-dimensional (2D) ^{129}Xe EXchange SpectroscopY (EXSY) NMR method. Using ^{129}Xe Selective Inversion Recovery (SIR) experiments, the rate for this exchange has been measured at 43 ± 6 s^{-1}.

2

I.　　　Introduction:

During the last two decades, Metal-Organic Frameworks (MOFs) materials have been widely studied because of their possible use in various applications ranging from gas storage to drug delivery. These compounds are hybrid materials built up from the three-dimensional association of metal clusters and organic ligands and exhibit interesting properties owning to their modular architecture and porosity[1, 2]. Amongst the large MOFs family, the specific case of the terephthalate-based MIL-53 [M(III)(1,4-benzendicarboxylate)] MOFs with M = Al, Fe, Ga, Cr, Sc or In[3-10] is of particular interest as these materials present massive flexibility and dynamic properties called the breathing effect. This latter is induced by changes in temperature[11] or external pressure[12, 13] as well as upon the presence of guest molecules (including xenon, water molecules, CO_2 or hydrocarbons)[14] and strongly depends on the nature of the linker[7, 15, 16] and the metal[17, 18]. This structural transition has been interpreted as a variation of MIL-53 structure between a large-pore (*lp*) form and a narrow-pore (*np*) one (see Figure 1).

a) MIL-53(Al)-*np* 　　　　　　　　　　　　　**b) MIL-53(Al)-*lp***

Figure 1. Views of the 3D structures of MIL-53(Al) materials in a) the *np* form and b) the *lp* one[19].

In this study, we focus on MIL-53(Al) since it combines low cost, density and toxicity and good thermal stability and is already produced at industrial scale under the name of Basolite® A100[19, 20]. The lattice framework of MIL-53(Al) and its structural transition has been investigated by powder X-ray diffraction (PXRD)[19, 21, 11, 22] and one-dimensional (1D) ^{1}H, ^{13}C and ^{27}Al solid-state NMR experiments[19, 23-28]. Furthermore, we have demonstrated recently how the measurement of the dephasing of ^{13}C signals under ^{13}C-^{27}Al dipolar couplings validates the crystal structures of the *lp* and *np* forms obtained from PXRD and confirms their rigidity[28]. The *lp-np* transition as function of the Xe pressure and the temperature has also been studied by ^{129}Xe NMR in MIL-53(Al)[29] and very recently in Cu-based MOF material (DUT-49)[30]. This technique allows to distinguish the *lp* and *np* forms of MIL-53(Al) and determine their relative proportion, however the spectral resolution of the reported

1D ^{129}Xe NMR spectra was limited by the NMR data acquisition under static conditions. Additionally, the motions of Xe atoms in the MIL-53(Al) pores and the exchange of Xe atoms between *lp* and *np* forms have not been investigated so far.

Here, the *lp-np* transition of MIL-53(Al) loaded with xenon is investigated using variable-temperature ^{129}Xe NMR under static and Magic-Angle Spinning (MAS) conditions and ^{1}H→^{129}Xe Cross-Polarization under MAS (CP-MAS) experiments are used to study the mobility of Xe atoms with respect to the pore walls. Finally, the exchange of Xe atoms between the *lp* and *np* forms is investigated using two-dimensional (2D) EXchange SpectroscopY (EXSY) experiments with the rate of exchange obtained by performing Selective Inversion Recovery (SIR) experiments.

II.   Experimental section:

II.1. Sample preparation for NMR measurements

MIL-53(Al) was synthesized according to the procedure reported in the literature[19]. 13 mg of MIL-53(Al) was activated under vacuum at 423 K overnight in a capillary. Xenon gas was added in the tube and condensed under liquid nitrogen. Then the tube was sealed, which gives an equilibrium pressure of ca. 5×10^4 Pa at room temperature. It should be noted that the powder was not squeezed into the capillary, and the sealing was performed as symmetrical as possible so that the rotor remains balanced and spun evenly. According to the adsorption isotherms[29], the xenon pressure inside the capillary varies very significantly with the temperature. For instance, the pressure is 4×10^2 Pa at 195 K, instead of 1.25×10^5 Pa at 323 K. Even at high temperature, there is no risk of overpressure and explosion of the capillary with 0.3 mm thick walls. We chose a capillary with an outer diameter of 3 mm, which exactly fitted into the 4 mm rotor. The rotor containing the capillary was spun without taking any special precaution.

II.2. NMR experiments

NMR spectra were recorded at 9.4 T (400 MHz for ^{1}H) using wide-bore Bruker BioSpin spectrometer equipped with either (i) an AVANCE-II console and a static double resonance HX probe or a 4 mm triple resonance HXY MAS probe (used in a double resonance mode) or (ii) an AVANCE-III HD console equipped with a 4 mm HXY triple resonance MAS probe (used in a double resonance mode). For all variable temperature NMR experiments, the samples were allowed to equilibrate at

the targeted temperature for 10 minutes. The temperature of the sample was controlled using a BCU-X Bruker system.

1D ^{129}Xe NMR spectra under static and MAS conditions at a rate ν_R = 10 kHz were acquired using a Direct Excitation sequence and a radio-frequency (rf) pulse at a nutation frequency of 62.5 kHz. The relaxation delay was τ_{RD} = 5 s and the number of scans was 512, which led to an experimental time of t_{exp} = 43 minutes. These experiments are quantitative since the ^{129}Xe longitudinal relaxation time, T_1 (^{129}Xe) is shorter than 1 s for all the temperatures and hence $\tau_{RD} > 5T_1$ (^{129}Xe). The molar fractions of Xe atoms adsorbed in the *lp* and *np* forms were calculated from the integrated intensities of their NMR signals in the 1D ^{129}Xe Direct Excitation NMR spectra under static conditions.

^{1}H $\rightarrow$ ^{129}Xe CPMAS were recorded at a MAS frequency of ν_R = 8 kHz using a recycle delay of τ_{RD} = 3 s, a 83 kHz 90° ^{1}H excitation pulse, a contact time of τ_{CP} = 8 ms, and rf nutation frequencies of 52 kHz and 60 kHz for ^{129}Xe and ^{1}H nuclei, respectively. SPINAL-64 (Small Phase Incremental Alternation with 64 steps)[31] ^{1}H decoupling of 83 kHz was applied during the acquisition of ^{129}Xe spectra. The number of scans was 800, which led to t_{exp} = 40 minutes.

2D ^{129}Xe EXSY experiments were performed at room temperature with ν_R = 10 kHz using rf pulses at a nutation frequency of 71 kHz. The 2D spectra result from averaging 512 transients for each of 30 t_1 increments with Δt_1 = 50 μs and τ_{RD} = 2 s. To ensure steady-state condition for the acquisition of the EXSY experiment, a train of pulses was applied prior the τ_{RD} delay to saturate the ^{129}Xe magnetization. This train used 20 pulses with rf-field amplitude of 81 kHz and a 20 ms delay between the consecutive pulses. The 2D EXSY spectra were acquired with mixing time (τ_{mix}) ranging from 5 μs to 1 s leading to experimental times ranging from t_{exp} = 10 hours 20 minutes to t_{exp} = 14 hours and 40 minutes. The pulse sequence is displayed in Fig. S1 of the Electronic Supporting Information File (ESI).

The T_1(^{129}Xe) times were measured at room temperature using standard non-selective inversion-recovery (NIR) experiments at ν_R = 10 kHz. The rf nutation frequency of ^{129}Xe $\pi/2$ and π pulses was 71 kHz and the relaxation delay was τ_{RD} = 10 s. The variable relaxation delay, τ, between the π and $\pi/2$ pulses was varied from 10 μs up to 5 s. The number of scans for these experiments was 512, which led to an experimental time of t_{exp} = 32 hours and 16 minutes. Selective Invertion Recovery (SIR) experiments were also conducted using the sequence shown in Fig. S3. A shaped π pulse selectively inverts one resonance[32, 33]. Here, we employed a Gaussian π pulse, with an rf peak amplitude of 1.6 kHz, a full width at half maximum of 6 kHz and a duration of 585 μs. This Gaussian pulse was truncated at 5 % of its maximum rf peak amplitude. It was applied on-resonance with the signal of the *np* form and the *lp* form in Fig. S4a and S4b respectively. The other parameters for the SIR experiments are identical to those of NIR ones.

The ^{1}H and ^{129}Xe chemical shifts were externally referenced to tetramethylsilane and gaseous xenon extrapolated to zero pressure, respectively and both set to 0 ppm. The sample temperature under MAS conditions was measured from the isotropic chemical shift of ^{207}Pb nuclei in Pb(NO$_3$)$_2$ [34] and all temperatures reported are actual sample temperatures.

The chemical shift parameters are defined according to the Haeberlen notation[35]

$$\delta_{iso} = \frac{1}{3}(\delta_{XX} + \delta_{YY} + \delta_{ZZ}) \tag{1}$$

$$\delta_{aniso} = \delta_{ZZ} - \delta_{iso} \tag{2}$$

$$\eta_{CSA} = \frac{\delta_{YY} - \delta_{XX}}{\delta_{ZZ} - \delta_{iso}} \tag{3}$$

where δ_{iso} denotes the isotropic chemical shift; δ_{XX}, δ_{YY}, and δ_{ZZ} are the principal components of the Chemical Shift Anisotropy (CSA) tensor ordered as $|\delta_{YY} - \delta_{iso}| \leq |\delta_{XX} - \delta_{iso}| \leq |\delta_{ZZ} - \delta_{iso}|$; δ_{aniso} corresponds to the anisotropic chemical shift and η_{CSA} is the asymmetry parameter of the CSA tensor.

The simulation of the 1D spectra were performed using DMfit software[36]. The exchange constant of the process k_{exch} in the case of the SIR experiments is measured by modeling the experimental data with the CIFIT program[32, 33].

III.   Results and discussion

III.1. 1D ^{129}Xe NMR spectra under static conditions
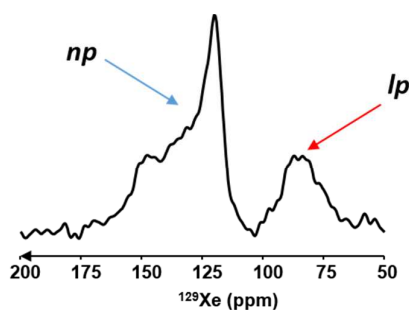
Figure 2. 1D ^{129}Xe direct excitation NMR spectrum of MIL-53(Al) loaded with xenon recorded under static conditions at 298 K.

The ^{129}Xe direct excitation NMR spectrum of MIL-53(Al) loaded with xenon under static conditions exhibits at 298 K two signals resonating at δ_{iso} of 128 and 90 ppm (Fig. 2), which are assigned to Xe atoms in the *np* and *lp* forms of MIL-53(Al), respectively[29]. This assignment agrees with the higher ^{129}Xe isotropic chemical shift in smaller pores for microporous solids[37-39]. The simulation of the spectrum (Fig. S5) yields the ^{129}Xe NMR parameters of the two forms (see Table 1). The *np* signal exhibits a relatively large δ_{aniso} value since the pores of this form have a rhomboid shape. On the contrary, no anisotropy is found for the *lp* form owing to the square shape of its pores (Fig. 1). The

6

higher symmetry of the pore cross-section in the case of the *lp* form induces a smaller constraint than in the *np* form (see Table 1).

Table 1. ^{129}Xe δ_{iso}, δ_{aniso} and η_{CSA} parameters, defined according to Eqs. 1 to 3, of the two forms of MIL-53(Al) at room temperature. Values were obtained from the simulation of the static lineshapes (Fig. S5).

	δ_{iso} / ppm	δ_{aniso} / ppm	η_{CSA}
np	128 ± 5	25 ± 5	0.2 ± 0.1
lp	90 ± 5	N/A	N/A

Figure S6 shows the variable temperature 1D ^{129}Xe direct excitation NMR spectra of MIL-53(Al) loaded with xenon between 327 to 237 K. When the temperature decreases from 301 to 237 K, the intensity of the *lp* signal decreases and almost totally vanish at 237 K. Such variation in signal intensity shows the conversion of *lp* into *np* form for decreasing temperature. Conversely, when the temperature is increased from 301 to 327 K, the signal intensity of the *np* form decreases and that of the *lp* form increases. The evolution of the fractions of xenon atoms adsorbed in the *lp* and *np* forms as function of the temperature is shown in Fig. 3.
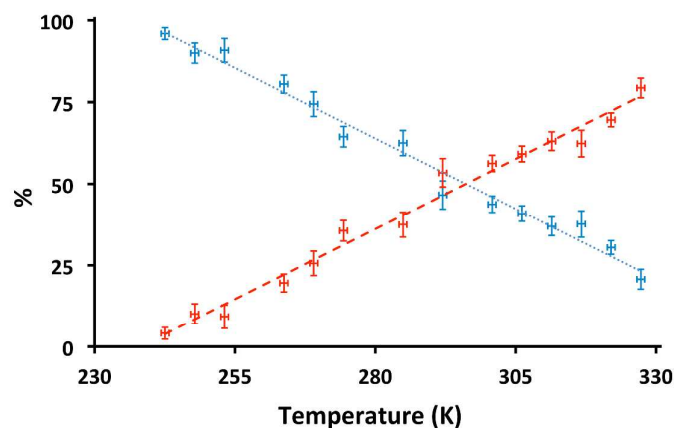
Figure 3. Molar fractions of xenon atoms adsorbed in the *np* (blue) and *lp* (red) forms for MIL-53(Al) loaded with gaseous xenon as function of the temperature. These were determined from the integrated intensities of the 1D ^{129}Xe NMR signals recorded under static conditions (see Fig. S6). The error bars were calculated according to Eq. S1 for the molar fraction while we estimated an error of 0.7 K for the temperature.

The coexistence of the two phases, for which a single phase is thermodynamically stable according to the phase diagram[40], has already been observed[29] and is potentially related to the kinetics of xenon adsorption. The presence of xenon equilibrates first the outer shell of the MIL-53(Al) particles. But, the diffusion of xenon through this shell is supposed to be slow. The cores of the

particles can be consequently away from thermodynamic equilibrium[41]. Such phenomenon would also explains the hysteresis observed for the absorption and the desorption of xenon in MIL-53(Al).[29] This behavior is not taken into account in the osmotic thermodynamic model, which assumes an homogeneous system at complete equilibrium.

The δ_{iso} shift of [129]Xe nuclei in the *np* form increases when the temperature decreases (Fig. S7). Such variation is typical for adsorbed xenon. The chemical shift originates from the interactions of xenon atoms with the pore surface and from the Xe-Xe interactions inside the pore[29, 39, 42]. The isotropic chemical shift of Xe atoms increases due to the reducing of shielding when in contact with the pore walls. In a sealed tube, the amount of adsorbed xenon does not vary much with temperature however the residence time of the xenon atoms on the surface increases when the temperature decreases. Because the xenon mobility is reduced at lower temperature, the average chemical shift increases with decreasing temperature. This increase is generally more important for small pores than for large pores since the residence time on the surface of small pores is longer compared to that on the large pores. It is not observed in the present case. In particular, the chemical shift of Xe adsorbed in the *lp* channels slightly decreases with the temperature (Fig. S7). This can be due to the slow exchange of Xe atoms between the *lp* and *np* channels. As the mobility of Xe atoms increases with the temperature and hence, the exchange between the two forms becomes faster.

III.2. 1D [129]Xe NMR spectra under MAS conditions
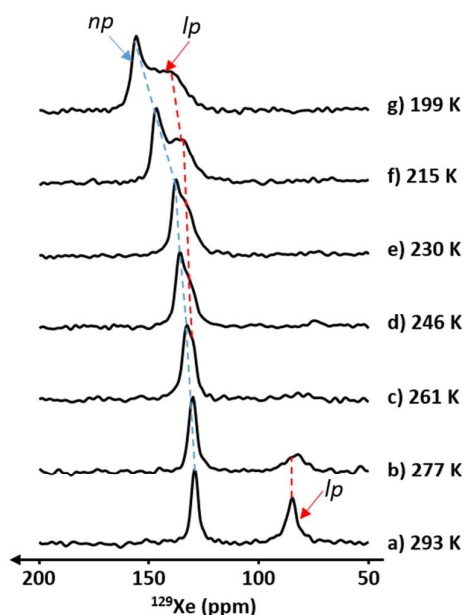
Figure 4. 1D ^{129}Xe direct excitation MAS NMR spectra of MIL-53(Al) loaded with xenon at v_R = 10 kHz and (a) 293, (b) 277, (c) 261, (d) 246, (e) 230, (f) 215 and (g) 199 K.

Figure 4a shows the 1D ^{129}Xe direct excitation MAS spectrum of MIL-53(Al) loaded with xenon at 293 K. The ^{129}Xe signals under MAS are narrower (especially for the *np* form) than under static conditions (compare Fig. 2 and 4a) since the MAS averages out the CSA. As observed in the static experiments, the intensity of the *lp* signal resonating around 90 ppm decreases with temperature and disappears at $T \leq 246$ K. Furthermore, the ^{129}Xe MAS spectra acquired at temperature ranging from 261 to 199 K exhibit two overlapping signals with $\delta_{iso} \geq 130$ ppm (Fig. 4b-g). They are assigned to the *np* and *lp* forms for the most and the least shifted signals, respectively. For instance, at 199 K, the isotropic chemical shift of the *np* signal is 155 ppm while the broad signal attributed to *lp* channels resonates at 144 ppm. This new *lp* signal is due to the reverse transformation (*np* → *lp*), that is consistent with the phase diagram of MIL-53(Al) in the presence of xenon gas which shows that the *np* form should transform back into *lp* one at low temperature.[40] This broad signal at 144 ppm is not observed in the static experiments because it is hidden by the broad anisotropic *np* signal. The evolution of the isotropic chemical shift of the *np* and the *lp* forms as a function of the temperature is reported in Fig. 5. Values were obtained from the simulation of the spectra under MAS conditions (Fig. S8).
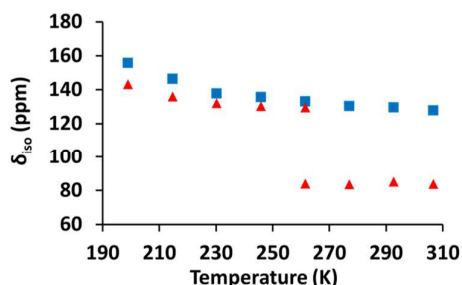

Figure 5. Evolution of δ_{iso} of the *np* form (blue squares) and *lp* form (red triangles) in MIL-53(Al) obtained from the 1D ^{129}Xe direct excitation NMR spectra of MIL-53(Al) loaded with xenon at v_R = 10 kHz.

III.3. 1D ^{1}H→^{129}Xe CPMAS spectra

1D ^{1}H→^{129}Xe CPMAS experiments have so far only been reported for clathrates and polymers[43-45]. Here, this experiment has been employed to probe the mobility of xenon atoms in the channels of the MIL-53(Al) compound. The 1D ^{1}H→^{129}Xe CPMAS spectra of MIL-53(Al) loaded with gaseous xenon at temperature ranging from 230 to 199 K are shown in Fig. 6. These spectra exhibit a single peak

assigned to the *np* phase. As already seen in Fig. 5, the isotropic chemical shift of the *np* signal increases as the temperature decreases owing to the increase of residence time of Xe atoms in the pores. Furthermore, as already observed in Fig. 4, the *np* signal is broader at 215 and 199 K with respect to 230 K. Such broadening results in decreased signal intensity. The absence of the *lp* signal in the 1D $^1H{\rightarrow}^{129}Xe$ CPMAS spectra indicates the high mobility of xenon atoms in the channels of the *lp* form since these motions average out the ^1H-^{129}Xe dipolar couplings. Furthermore, the signal intensity of the 1D $^1H{\rightarrow}^{129}Xe$ CPMAS signal of *np* site reaches a maximum after a 8 or 10 ms contact time (Fig. S9). By comparison, it has been shown that CPMAS transfers between surface protons and adsorbed ^{129}Xe nuclei in the absence of motions only requires contact time of 2 ms approximately[46]. The longer contact time required here suggests that the xenon atoms adsorbed in the channels of the *np* form of MIL-53(Al) exhibit significant motion on time scales faster than a few milliseconds at 199 K.
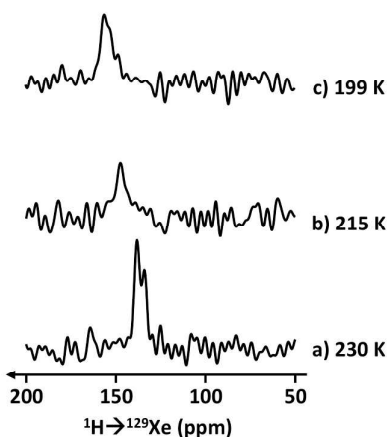
Figure 6. 1D $^1H{\rightarrow}^{129}Xe$ CPMAS spectra of the *np* form of the MIL-53(Al) loaded with xenon and recorded at ν_R = 8 kHz and (a) 230 K, (b) 215 K and (c) 199 K.

III.4. 2D ^{129}Xe EXSY experiments

2D ^{129}Xe EXSY experiments have already been employed to study the chemical exchanges between distinct ^{129}Xe environments in MOFs[42]. Here, this experiment has been employed to investigate the exchange between the *np* and *lp* ^{129}Xe signals. Figure 7 shows the 2D ^{129}Xe EXSY spectrum of MIL-53(Al) loaded with xenon at room temperature. The presence of cross-peaks between the *np* and *lp* signals proves the exchange of xenon atoms between the two forms of the MIL-53(Al). Hence, at room temperature, the xenon atoms diffuse between the channels of *np* and *lp* domains of MIL-53(Al) for a time scale higher than hundreds of milliseconds.

By measuring the intensity of the NMR signals in the 2D EXSY MAS spectra recorded for different τ_{mix} values (see Figs. S10 and S11), we estimate that the exchange rate of xenon atoms between the

10

channels of the *lp* and *np* forms is in the order of 20 s^{-1}. This value is comparable to exchange rates of xenon atoms between the pores of NaX and NaY zeolite particles[47] and in zinc-based MOFs[42].
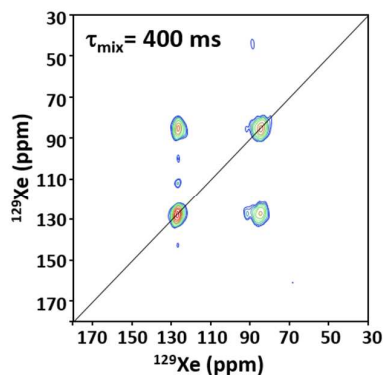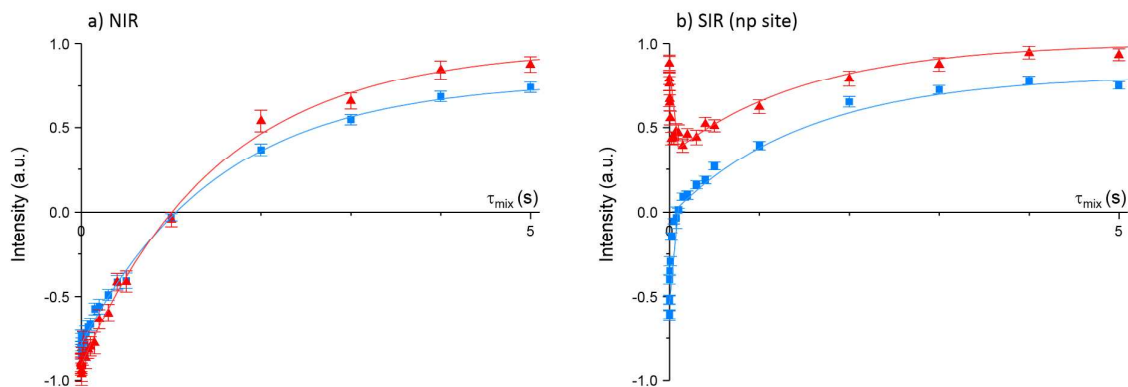

Figure 7. 2D ^{129}Xe MAS EXSY spectrum of MIL-53(Al) loaded with xenon and recorded at ν_R = 10 kHz and room temperature with τ_{mix} = 400 ms.

III.5. SIR 1D MAS results

The SIR 1D MAS experiment is an accurate and rapid method to measure the exchange rate between two sites.[32, 33] Introduced for the study of chemical exchange in solution, it has been recently applied to probe the kinetics of lithium mobility in battery systems[48]. The determination of the exchange rate is faster using SIR experiments than 2D EXSY ones since the SIR experiment can be acquired in approximately the same time as a single 2D EXSY spectrum. Furthermore, the exchange rates determined from SIR experiments are usually more accurate than those extracted from 2D EXSY spectra as the EXSY intensities can be distorted by the t_1 ridge caused by the longitudinal relaxation during the EXSY sequence and these t_1 ridges cannot be eliminated by the phase cycling.[49, 50]

The Journal of Physical Chemistry

Page 12 of 16

1
2
3
4
5
6
7
8
9
10
11
12
13
14
15
16
17
18
19
20
21
22
23
24
25
26
27
28
29
30
31
32
33
34
35
36
37
38
39
40
41
42
43
44
45
46
47
48
49
50
51
52
53
54
55
56
57
58
59
60

Figure 8. (a) NIR and (b) SIR experiments on MIL-53(Al) loaded with xenon at ν_R = 10 kHz and room temperature. For SIR experiment, the *np* signal was selectively inverted. The experimental signal intensities are displayed as symbol (blue squares for *np* form and red triangles for *lp* one). The best fit curves are displayed as continuous lines (blue for *np* form and red for *lp* one). The error bars were taken as the noise standard deviation of the signals.

The $T_1(^{129}Xe)$ values of *np* and *lp* signals of MIL-53(Al) loaded with xenon were determined at room temperature from NIR experiments (see Fig. 8a). In order to estimate the exchange rate, we then carried out SIR experiments under similar conditions. As the *lp* resonance is broader than the *np* one, the selective inversion of the *np* signal is more efficient than the *lp* one (see Fig. S4). The SIR data using a selective inversion of the *np* signal is shown in Fig. 8b. The chemical exchange between the two ^{129}Xe environments causes (i) a rapid decrease of the *lp* signal as well as (ii) a simultaneous increase of the *np* one for short τ delay (τ < 0.2 s). The fit of SIR data by fixing $T_1(^{129}Xe)$ parameters to their values determined from NIR yields k_{exch} = 43 ± 6 s^{-1}. This value agrees with the rough estimate derived from the 2D EXSY experiments.

Conclusion

We have investigated the *np-lp* transition of MIL-53(Al) loaded with gaseous xenon and the mobility of the xenon atoms in this flexible MOF. ^{129}Xe direct excitation NMR experiments under static and MAS conditions have shown that as the temperature decreases, the amount of *lp* form decreases and almost vanishes at 237 K and increases again for $T \leq$ 230 K. Such trends are consistent with the previously reported phase diagram[40]. Nevertheless, a major difference lies in the coexistence of the *lp* and *np* phases for most investigated temperatures. This heterogeneity of the system is ascribed to the kinetics of xenon adsorption. $^1H \rightarrow ^{129}Xe$ CPMAS experiments show the restricted mobility of xenon atoms in the *np* channels at $T \leq$ 230 K. Nevertheless, the long required contact times indicates that xenon atoms in such environment move on timescale faster than a few milliseconds. 2D EXSY spectra demonstrate the exchange of xenon atoms between the two forms of MIL-53(Al) at room temperature. The rate for this exchange was measured by SIR and is equal to 43 ± 6 s^{-1}.

Supporting Information. The supporting information contains the pulse sequences used in the manuscript, 1D ^{129}Xe spectra of MIL-53(Al) recorded under static conditions, variation of the ^{129}Xe isotropic chemical shifts as function of the temperature, 1D $^1H \rightarrow ^{129}Xe$ CPMAS build-up curves recorded at 153 K, 2D ^{129}Xe EXSY spectra and the corresponding theory.

1
2
3
4
5
6
7
8
9
10
11
12
13
14
15
16
17
18
19
20
21
22
23
24
25
26
27
28
29
30
31
32
33
34
35
36
37
38
39
40
41
42
43
44
45
46
47
48
49
50
51
52
53
54
55
56
57
58
59
60

References:

1.   Long, J. R.; Yaghi, O. M., Themed Issue: Metal-Organic Frameworks. *Chem. Soc. Rev.* **2009,** *38*, 1207-1508.
2.   Zhou, H. C.; Long, J. R.; Yaghi, O. M., Introduction to Metal-Organic Frameworks. *Chem. Rev.* **2012,** *112*, 673-1268.
3.   Volkringer, C.; Loiseau, T.; Guillou, N.; Férey, G.; Elkaim, E.; Vimont, A., XRD and IR Structural Investigations of a Particular Breathing Effect in the MOF-type Gallium Terephthalate MIL-53(Ga). *Dalton Trans.* **2009**, *12*, 2241-2249.
4.   Kolokolov, D. I.; Jobic, H.; Stepanov, A. G.; Guillerm, V.; Devic, T.; Serre, C.; Férey, G., Dynamics of Benzene Rings in MIL-53(Cr) and MIL-47(V) Frameworks Studied by ^{2}H NMR Spectroscopy. *Angew. Chem.-Int. Ed.* **2010,** *49*, (28), 4791-4794.
5.   Coudert, F. X.; Ortiz, A. U.; Haigis, V.; Bousquet, D.; Fuchs, A. H.; Ballandras, A.; Weber, G.; Bezverkhyy, I.; Geolfroy, N.; Bellat, et al., Water Adsorption in Flexible Gallium-Based MIL-53 Metal-Organic Framework. *J. Phys. Chem. C* **2014,** *118*, 5397-5405.
6.   Loiseau, T.; Volkringer, C.; Haouas, M.; Taulelle, F.; Férey, G., Crystal Chemistry of Aluminium Carboxylates: From Molecular Species Towards Porous Infinite Three-Dimensional Networks. *Comptes Rendus Chimie* **2015,** *18*, 1350-1369.
7.   Reinsch, H.; Pillai, R. S.; Siegel, R.; Senker, J.; Lieb, A.; Maurin, G.; Stock, N., Structure and Properties of Al-MIL-53-ADP, a Breathing MOF Based on the Aliphatic Linker Molecule Adipic Acid. *Dalton Trans.* **2016,** *45*, 4179-4186.
8.   Serre, C.; Millange, F.; Thouvenot, C.; Nogues, M.; Marsolier, G.; Louer, D.; Férey, G., Very Large Breathing Effect in the First Nanoporous Chromium(III)-Based Solids: MIL-53 or Cr-III(OH).{O_2C-C_6H_4-CO_2}.{HO_2C-C_6H_4-CO_2H}$_x$.H_2O_y. *J. Am. Chem. Soc.* **2002,** *124*, 13519-13526.
9.   Ibarra, I. A.; Lin, X.; Yang, S.; Blake, A. J.; Walker, G. S.; Barnett, S. A.; Allan, D. R.; Champness, N. R.; Hubberstey, P.; Schroeder, M., Structures and H_2 Adsorption Properties of Porous Scandium Metal-Organic Frameworks. *Chem. Eur. J.* **2010,** *16*, 13671-13679.
10.   Anokhina, E. V.; Vougo-Zanda, M.; Wang, X. Q.; Jacobson, A. J., In(OH)BDC.0.75BDCH$_2$ (BDC = benzenedicarboxylate), a Hybrid Inorganic-Organic Vernier Structure. *J. Am. Chem. Soc.* **2005,** *127*, 15000-15001.
11.   Liu, Y.; Her, J.-H.; Dailly, A.; Ramirez-Cuesta, A. J.; Neumann, D. A.; Brown, C. M., Reversible structural transition in MIL-53 with large temperature hysteresis. *J. Am. Chem. Soc.* **2008,** *130*, 11813-11818.
12.   Yot, P. G.; Vanduyfhuys, L.; Alvarez, E.; Rodriguez, J.; Itie, J. P.; Fabry, P.; Guillou, N.; Devic, T.; Beurroies, I.; Llewellyn, et al., Mechanical Energy Storage Performance of an Aluminum Fumarate Metal-Organic Framework. *Chem. Sci.* **2016,** *7*, 446-450.
13.   Beurroies, I.; Boulhout, M.; Llewellyn, P. L.; Kuchta, B.; Férey, G.; Serre, C.; Denoyel, R., Using Pressure to Provoke the Structural Transition of Metal-Organic Frameworks. *Angew. Chem.-Int. Ed.* **2010,** *49*, 7526-7529.

14.	Llewellyn, P. L.; Maurin, G.; Devic, T.; Loera-Serna, S.; Rosenbach, N.; Serre, C.; Bourrelly, S.; Horcajada, P.; Filinchuk, Y.; Férey, G., Prediction of the Conditions for Breathing of Metal-Organic Framework Materials Using a Combination of X-Ray Powder Diffraction, Microcalorimetry, and Molecular Simulation. *J. Am. Chem. Soc.* **2008,** *130*, 12808-12814.

15.	Loiseau, T.; Mellot-Draznieks, C.; Muguerra, H.; Férey, G.; Haouas, M.; Taulelle, F., Hydrothermal Synthesis and Crystal Structure of a New Three-Dimensional Aluminum-Organic Framework MIL-69 with 2,6-Naphthalenedicarboxylate (ndc), Al(OH)(ndc).H_2O *Comptes Rendus Chimie* **2005,** *8*, 765-772.

16.	Senkovska, I.; Hoffmann, F.; Froba, M.; Getzschmann, J.; Bohlmann, W.; Kaskel, S., New Highly Porous Aluminium Based Metal-Organic Frameworks: Al(OH)(ndc) (ndc=2,6-Naphthalene dicarboxylate) and Al(OH)(bpdc) (bpdc=4,4'-biphenyl dicarboxylate). *Microporous Mesoporous Mater.* **2009,** *122*, 93-98.

17.	Liu, Y. Y.; Leus, K.; Grzywa, M.; Weinberger, D.; Strubbe, K.; Vrielinck, H.; Van Deun, R.; Volkmer, D.; Van Speybroeck, V.; Van der Voort, P., Synthesis, Structural Characterization, and Catalytic Performance of a Vanadium-Based Metal-Organic Framework (COMOC-3). *Eur. J. Inorg. Chem.* **2012**, 2819-2827.

18.	Millange, F.; Guillou, N.; Walton, R. I.; Greneche, J. M.; Margiolaki, I.; Fereya, G., Effect of the Nature of the Metal on the Breathing Steps in MOFs with Dynamic Frameworks. *Chem. Commun.* **2008**, (39), 4732-4734.

19.	Loiseau, T.; Serre, C.; Huguenard, C.; Fink, G.; Taulelle, F.; Henry, M.; Bataille, T.; Férey, G., A Rationale for the Large Breathing of the Porous Aluminum Terephthalate (MIL-53) upon Hydration. *Chem. Eur. J.* **2004,** *10*, 1373-1382.

20.	Gaab, M.; Trukhan, N.; Maurer, S.; Gummaraju, R.; Muller, U., The Progression of Al-Based Metal-Organic Frameworks - From Academic Research to Industrial Production and Applications. *Microporous Mesoporous Mater.* **2012,** *157*, 131-136.

21.	Horcajada, P.; Serre, C.; Maurin, G.; Ramsahye, N. A.; Balas, F.; Vallet-Regi, M.; Sebban, M.; Taulelle, F.; Férey, G., Flexible Porous Metal-Organic Frameworks for a Controlled Drug Delivery. *J. Am. Chem. Soc.* **2008,** *130*, 6774-6780.

22.	Guillou, N.; Millange, F.; Walton, R. I., Rapid and Reversible Formation of a Crystalline Hydrate of a Metal-Organic Framework Containing a Tube of Hydrogen-Bonded Water. *Chem. Commun.* **2011,** *47*, 713-715.

23.	Ibrahim, B.; Lucier, B. E. G.; Xu, J.; He, P.; Huang, Y. N., Investigating Adsorption of Organic Compounds in Metal-Organic Framework MIL-53. *Can. J. Chem.* **2015,** *93*, 960-969.

24.	Liu, J.; Zhang, F.; Zou, X. Q.; Yu, G. L.; Zhao, N.; Fan, S. J.; Zhu, G. S., Environmentally Friendly Synthesis of Highly Hydrophobic and Stable MIL-53 MOF Nanomaterials. *Chem. Commun.* **2013,** *49*, 7430-7432.

25.	Jiang, Y. J.; Huang, J.; Marx, S.; Kleist, W.; Hunger, M.; Baiker, A., Effect of Dehydration on the Local Structure of Framework Aluminum Atoms in Mixed Linker MIL-53(Al) Materials Studied by Solid-State NMR Spectroscopy. *J. Phys. Chem. Lett.* **2010,** *1*, 2886-2890.

26.	Lieder, C.; Opelt, S.; Dyballa, M.; Henning, H.; Klemm, E.; Hunger, M., Adsorbate Effect on $AlO_4(OH)_2$ Centers in the Metal-Organic Framework MIL-53 Investigated by Solid-State NMR Spectroscopy. *J. Phys. Chem. C* **2010,** *114*, 16596-16602.

27.	Goesten, M. G.; Juan-Alcaniz, J.; Ramos-Fernandez, E. V.; Gupta, K.; Stavitski, E.; van Bekkum, H.; Gascon, J.; Kapteijn, F., Sulfation of Metal-Organic Frameworks: Opportunities for Acid Catalysis and Proton Conductivity. *J. Catal.* **2011,** *281*, 177-187.

28.	Giovine, R.; Volkringer, C.; Trébosc, J.; Amoureux, J. P.; Loiseau, T.; Lafon, O.; Pourpoint, F., NMR Crystallography to Probe the Breathing Effect of the MIL-53(Al) Metal-Organic Framework Using Solid-State NMR Measurements of [13]C-[27]Al Distances. *Acta Cryst C* **2017,** *73*, 176-183.

29.	Springuel-Huet, M. A.; Nossov, A.; Adem, Z.; Guenneau, F.; Volkringer, C.; Loiseau, T.; Férey, G.; Gedeon, A., [129]Xe NMR Study of the Framework Flexibility of the Porous Hybrid MIL-53(Al). *J. Am. Chem. Soc.* **2010,** *132*, 11599-11607.

14

30.   Schaber, J.; Krause, S.; Paasch, S.; Senkovska, I.; Bon, V.; Tobbens, D. M.; Wallacher, D.; Kaskel, S.; Brunner, E., In Situ Monitoring of Unique Switching Transitions in the Pressure Amplifying Flexible Framework Material DUT-49 by High-Pressure [129]Xe NMR Spectroscopy. *J. Phys. Chem. C* **2017,** *121*, 5195-5200.

31.   Fung, B. M.; Khitrin, A. K.; Ermolaev, K., An Improved Broadband Decoupling Sequence for Liquid Crystals and Solids. *J. Magn. Reson.* **2000,** *142*, 97-101.

32.   Bain, A. D.; Fletcher, D. A., Selective-Inversion Experiments Applied to Chemical Exchange in Coupled Spin Systems. *Mol. Phys.* **1998,** *95*, 1091-1098.

33.   Bain, A. D., Chemical exchange in NMR. *Prog. Nucl. Magn. Reson. Spectrosc.* **2003,** *43*, 63-103.

34.   Bielecki, A.; Burum, D. P., Temperature-Dependence of [207]Pb MAS Spectra of Solid Lead Nitrate - an Accurate, Sensitive Thermometer for Variable-Temperature MAS. *J. Magn. Reson Series A* **1995,** *116*, 215-220.

35.   Schmidt-Rohrr, K.; Spiess, H. W., Multidimensional Solid-State NMR and Polymers. *Hartcourt Brace & Company: London 1999*.

36.   Massiot, D.; Fayon, F.; Capron, M.; King, I.; Le Calve, S.; Alonso, B.; Durand, J. O.; Bujoli, B.; Gan, Z. H.; Hoatson, G., Modelling One- and Two-Dimensional Solid-State NMR Spectra. *Magn. Reson. Chem.* **2002,** *40*, 70-76.

37.   Demarquay, J.; Fraissard, J., [129]Xe NMR of Xenon Adsorbed on Zeolites - Relationship Between the Chemical Shift and the Void Space. *Chem. Phys. Lett.* **1987,** *136*, 314-318.

38.   Hoffmann, H. C.; Debowski, M.; Muller, P.; Paasch, S.; Senkovska, I.; Kaskel, S.; Brunner, E., Solid-State NMR Spectroscopy of Metal-Organic Framework Compounds (MOFs). *Materials* **2012,** *5*, ,2537-2572.

39.   Bonardet, J. L.; Fraissard, J.; Gedeon, A.; Springuel-Huet, M. A., Nuclear Magnetic Resonance of Physisorbed [129]Xe Used as a Probe to Investigate Porous Solids. *Cat. Rev.-Sci. Eng.* **1999,** *41*, 115-225.

40.   Boutin, A.; Springuel-Huet, M. A.; Nossov, A.; Gedeon, A.; Loiseau, T.; Volkringer, C.; Ferey, G.; Coudert, F. X.; Fuchs, A. H., Breathing Transitions in MIL-53(Al) Metal-Organic Framework Upon Xenon Adsorption. *Angew. Chem-Int. Ed.* **2009,** *48*, 8314-8317.

41.   Weber, G.; Bezverkhyy, I.; Bellat, J.-P.; Ballandras, A.; Ortiz, G.; Chaplais, G.; Patarin, J.; Coudert, F.-X.; Fuchs, A. H.; Boutin, A., Mechanism of Water Adsorption in the Large Pore Form of the Gallium-Based MIL-53 Metal-Organic Framework. *Micropor. Mesopor. Mater.* **2016,** *222*, 145-152.

42.   Ooms, K. J.; Wasylishen, R. E., [129]Xe NMR Study of Xenon in Iso-Reticular Metal-Organic Frameworks. *Microporous Mesoporous Mater.* **2007,** *103*, 341-351.

43.   Ripmeester, J. A., Nuclear Shielding of Trapped Xenon Obtained by Proton-Enhanced, Magic-Angle Spinning [129]Xe NMR Spectroscopy. *J. Am. Chem. Soc.* **1982,** *104,* 289-290.

44.   Lee, C. T.; Yang, W. T.; Parr, R. G., Development of the Colle-Salvetti Correlation-Energy Formula into a Functional of the Electron Density. *Phys. Rev. B* **1988,** *37*, 785-789.

45.   Mansfeld, M.; Veeman, W. S., ^{1}H-[129]Xe Double-Resonance NMR in a Polymer Blend. *Chem. Phys. Lett.* **1994,** *222*, 422-424.

46.   Gaede, H. C.; Song, Y. Q.; Taylor, R. E.; Munson, E. J.; Reimer, J. A.; Pines, A., High-Field Cross-Polarization NMR from Laser-Polarized Xenon to Surface Nuclei. *Appl. Magn. Reson.* **1995,** *8*, 373-384.

47.   Moudrakovski, I. L.; Ratcliffe, C. I.; Ripmeester, J. A., Application of [129]Xe 2D EXSY NMR to Intraparticle and Interparticle Exchange in Zeolites. *Appl. Magn. Reson.* **1995,** *8*, 385-399.

48.   Davis, L. J. M.; Heinmaa, I.; Goward, G. R., Study of Lithium Dynamics in Monoclinic $Li_3Fe_2(PO_4)_3$ using [6]Li VT and 2D Exchange MAS NMR Spectroscopy. *Chem. Mater.* **2010,** *22*, 769-775.

49.   Willem, R., 2D NMR applied to dynamics stereochemical problems. *Progr. Nucl. Magn. Reson. Spectrosc.* **1987,** *20*, 1-94.

50.   Orrell, K. G.; Sik, V.; Stephenson, D., Quantitative Investigations of Molecular Stereodynamics by 1D and 2D NMR Methods. *Prog. Nucl. Magn. Reson. Spectrosc.* **1990,** *22*, 141-208.

TOC

$Xe_{(g)}$

$43 \pm 6\ s^{-1}$